Acta Cryst E CRYSTALLOGRAPHIC COMMUNICATIONS

ISSN 2056-9890

Crystal structure, Hirshfeld surface analysis and interaction energy and DFT studies of methyl 4-[3,6-bis(pyridin-2-yl)pyridazin-4-yl]benzoate

Mouad Filali,[a] Lhoussaine El Ghayati,[b] Tuncer Hökelek,[c] Joel T. Mague,[d] Abdessalam Ben-Tama,[a] El Mestafa El Hadrami[a] and Nada Kheira Sebbar[e,b]*

[a]Laboratoire de Chimie Organique Appliquée, Université Sidi Mohamed Ben Abdallah, Faculté des Sciences et Techniques, Route d'immouzzer, BP 2202, Fez, Morocco, [b]Laboratoire de Chimie Organique Hétérocyclique URAC 21, Pôle de Compétence Pharmacochimie, Av. Ibn Battouta, BP 1014, Faculté des Sciences, Université Mohammed V, Rabat, Morocco, [c]Department of Physics, Hacettepe University, 06800 Beytepe, Ankara, Turkey, [d]Department of Chemistry, Tulane University, New Orleans, LA 70118, USA, and [e]Laboratoire de Chimie Appliquée et Environnement, Equipe de Chimie Bioorganique Appliquée, Faculté des sciences, Université Ibn Zohr, Agadir, Morocco. *Correspondence e-mail: nadouchsebbarkheira@gmail.com

Received 30 September 2019
Accepted 8 October 2019

Edited by A. J. Lough, University of Toronto, Canada

Keywords: crystal structure; pyridazine; pyridine; hydrogen bond; C—H···π(ring) interaction; Hirshfeld surface.

CCDC reference: 1958277

Supporting information: this article has supporting information at journals.iucr.org/e

The title compound, $C_{22}H_{16}N_4O_2$, contains two pyridine rings and one methoxycarbonylphenyl group attached to a pyridazine ring which deviates very slightly from planarity. In the crystal, ribbons consisting of inversion-related chains of molecules extending along the *a*-axis direction are formed by $C—H_{Mthy}\cdots O_{Carbx}$ (Mthy = methyl and Carbx = carboxylate) hydrogen bonds. The ribbons are connected into layers parallel to the *bc* plane by $C—H_{Bnz}\cdots\pi$(ring) (Bnz = benzene) interactions. The Hirshfeld surface analysis of the crystal structure indicates that the most important contributions for the crystal packing are from H···H (39.7%), H···C/C···H (27.5%), H···N/N···H (15.5%) and O···H/H···O (11.1%) interactions. Hydrogen-bonding and van der Waals interactions are the dominant interactions in the crystal packing. Computational chemistry indicates that in the crystal, $C—H_{Mthy}\cdots O_{Carbx}$ hydrogen-bond energies are 62.0 and 34.3 kJ mol^{-1}, respectively. Density functional theory (DFT) optimized structures at the B3LYP/6-311G(d,p) level are compared with the experimentally determined molecular structure in the solid state. The HOMO–LUMO behaviour was elucidated to determine the energy gap.

1. Chemical context

3,6-Bis(pyridin-2-yl)pyridazine derivatives are a versatile class of nitrogen-containing heterocyclic compounds and they constitute useful intermediates in organic syntheses. Also, this nucleus is one of the important ligands in the field of coordination chemistry research. 5-[3,6-Bis(pyridin-2-yl)pyridazine-4-yl]-2′-deoxyuridine-5′-*O*-triphosphate can be used as a potential substrate for fluorescence detection and imaging of DNA (Kore *et al.*, 2015). Systems containing this moiety also showed remarkable corrosion inhibition (Khadiri *et al.*, 2016). Heterocyclic molecules such as 3,6-bis(pyridin-2-yl)-1,2,4,5-tetrazine have been used in transition-metal chemistry (Kaim & Kohlmann, 1987); this tetrazine is a bidentate chelating ligand popular in coordination chemistry and complexes of a wide range of metals, including iridium and palladium (Tsukada *et al.*, 2001). As a continuation of our research in the field of substituted 3,6-bis(pyridin-2-yl)pyridazine (Filali *et al.*, 2019*a*,*b*), we report herein the synthesis, the molecular and crystal structures, along with the Hirshfeld surface analysis, the intermolecular interaction energies and the density functional theory (DFT) computational calculations carried out at

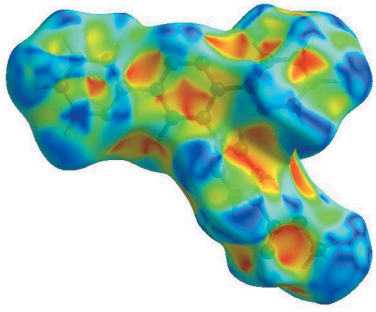

Table 1
Hydrogen-bond geometry (Å, °).

*Cg*1 is the centroid of pyridyl ring *A* (atoms N1/C1–C5).

D—H···*A*	*D*—H	H···*A*	*D*···*A*	*D*—H···*A*
C19—H19···*Cg*1^{i}	0.967 (15)	2.876 (15)	3.5715 (13)	129.8 (12)
C22—H22*B*···O1^{iv}	0.964 (19)	2.598 (19)	3.5407 (19)	165.8 (14)
C22—H22*C*···O1^{v}	0.959 (19)	2.536 (19)	3.4924 (16)	174.8 (15)

Symmetry codes: (i) $-x+1, -y+1, -z+1$; (iv) $-x+1, -y+2, -z+2$; (v) $x-1, y, z$.

the B3LYP/6-311G(d,p) level for a new 3,6-bis(pyridin-2-yl)pyridazine, namely, methyl 4-[3,6-bis(pyridin-2-yl)pyridazin-4-yl]benzoate, (I).

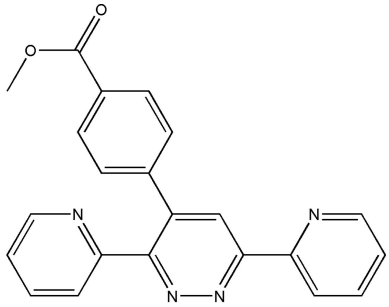

(I)

2. Structural commentary

The title compund contains two pyridine rings and one methoxycarbonylphenyl group attached to a pyridazine ring, where the central pyridazine ring, *B* (atoms N2/N3/C6–C9), deviates slightly from planarity by ±0.021 (1) Å (r.m.s. deviation = 0.0134 Å) (Fig. 1). The planes of the pyridine rings, *A* (N1/C1–C5) and *C* (N4/C10–C14), are inclined to the mean plane of the pyridazine ring, *B*, by 18.68 (6) and 38.40 (6)°, respectively, while the benzene ring, *D* (C15–C20), is inclined to it by 62.59 (5)°. The pyridine and benzene rings are oriented at dihedral angles of *A*/*C* = 25.16 (4)°, *A*/*D* = 48.94 (4)° and *C*/*D* = 59.13 (4)°. The plane of the carboxyl group (defined by atoms C18/C21/O1/O2) is twisted out of the plane of the benzene ring, *D*, by 22.88 (5)°.

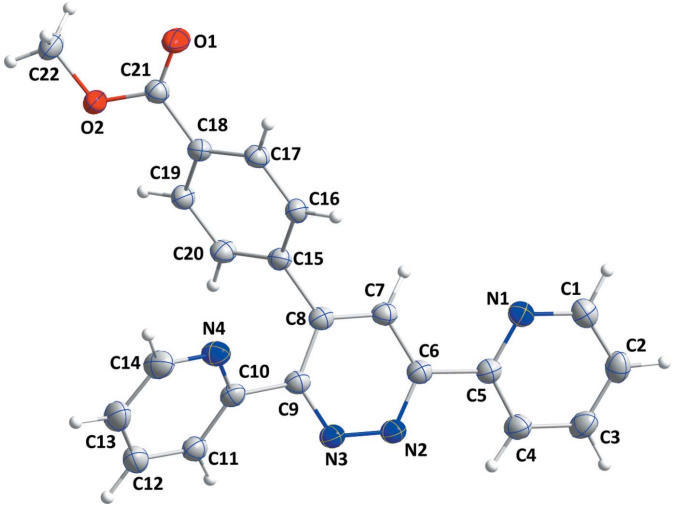

Figure 1
The molecular structure of the title compound with the atom-numbering scheme. Displacement ellipsoids are drawn at the 50% probability level.

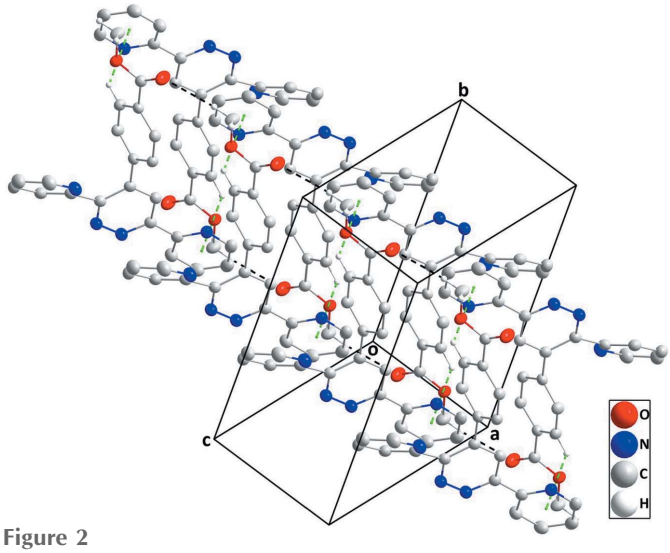

Figure 2
A partial packing diagram showing two chains connnected by C—H···π(ring) interactions (green dashed lines). The C—H_{Mthy}···O_{Carbx} (Mthy = methyl and Carbx = carboxylate) hydrogen bonds are shown as black dashed lines.

3. Supramolecular features

In the crystal, chains of molecules extending along the *a*-axis direction are formed by C22—H22*C*···O1^{v} hydrogen bonds (Table 1). Inversion-related chains are connected into ribbons by C22—H22*B*···O1^{iv} hydrogen bonds (Table 1) and the ribbons are joined into stepped layers approximately parallel to (01$\bar{1}$) by inversion-related pairs of C19—H19···*Cg*1^{i} interactions, where *Cg*1 is the centroid of pyridine ring *A* (Table 1 and Fig. 2). The Hirshfeld surface analysis of the crystal structure indicates that the most important contributions for the crystal packing are from H···H (39.7%), H···C/C···H (27.5%), H···N/N···H (15.5%) and O···H/H···O

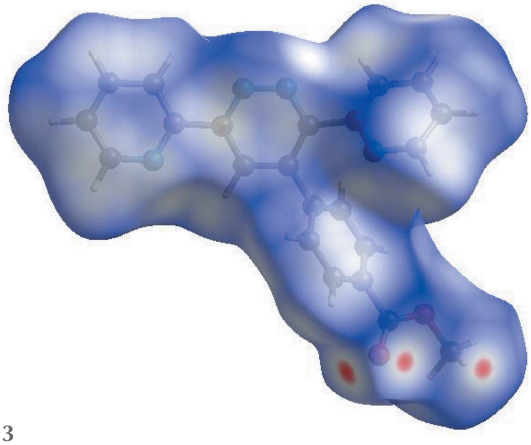

Figure 3
View of the three-dimensional Hirshfeld surface of the title compound plotted over d_{norm} in the range −0.1417 to 1.3796 a.u.

Table 2
Selected interatomic distances (Å).

O2···C3^{i}	3.4089 (16)	N4···H14^{viii}	2.931 (18)
O1···H12^{ii}	2.765 (16)	C1···C6^{iii}	3.4447 (17)
O1···H22*A*	2.573 (18)	C1···C7^{iii}	3.5272 (17)
O1···H22*B*	2.660 (18)	C2···C17^{ix}	3.4292 (18)
O1···H22*C*^{iii}	2.537 (19)	C3···C3^{x}	3.5516 (18)
O1···H22*B*^{iv}	2.598 (18)	C6···C11^{iii}	3.3751 (16)
O1···H17	2.611 (14)	C10···C20	3.3022 (16)
O2···H17^{v}	2.773 (13)	C11···C22^{vii}	3.4630 (18)
O2···H19	2.462 (14)	C14···C17^{viii}	3.4960 (18)
N1···C9^{iii}	3.4168 (15)	C14···C16^{viii}	3.4987 (18)
N2···C1^{v}	3.4404 (16)	C1···H19^{i}	2.926 (16)
N4···C20	3.2459 (16)	C6···H11^{iii}	2.924 (15)
N4···C15	2.8825 (15)	C7···H1^{v}	2.988 (17)
N4···C16	3.4362 (16)	C11···H22*A*^{vii}	2.964 (18)
N1···H20^{iii}	2.750 (15)	C16···H14^{viii}	2.891 (17)
N1···H7	2.553 (14)	C17···H2^{ix}	2.898 (18)
N2···H4^{vi}	2.710 (17)	C18···H2^{ix}	2.822 (18)
N2···H4	2.511 (17)	H3···H11^{vi}	2.53 (2)
N3···H11	2.644 (13)	H4···H4^{vi}	2.43 (3)
N3···H22*A*^{vii}	2.713 (17)	H7···H20^{iii}	2.43 (2)
N3···H3^{vi}	2.644 (18)	H16···H19^{iii}	2.57 (2)

Symmetry codes: (i) $-x+1, -y+1, -z+1$; (ii) $x+1, y+1, z$; (iii) $x+1, y, z$; (iv) $-x+1, -y+2, -z+2$; (v) $x-1, y, z$; (vi) $-x+1, -y, -z+1$; (vii) $x, y-1, z$; (viii) $-x+1, -y+1, -z+2$; (ix) $-x+2, -y+1, -z+1$; (x) $-x+2, -y, -z+1$.

(11.1%) interactions. Hydrogen-bonding and van der Waals interactions are the dominant interactions in the crystal packing.

4. Hirshfeld surface analysis

In order to visualize the intermolecular interactions in the crystal of the title compound, a Hirshfeld surface (HS) analysis (Hirshfeld, 1977; Spackman & Jayatilaka, 2009) was carried out by using *CrystalExplorer* (Version 17.5; Turner *et al.*, 2017). In the HS plotted over d_{norm} (Fig. 3), the white

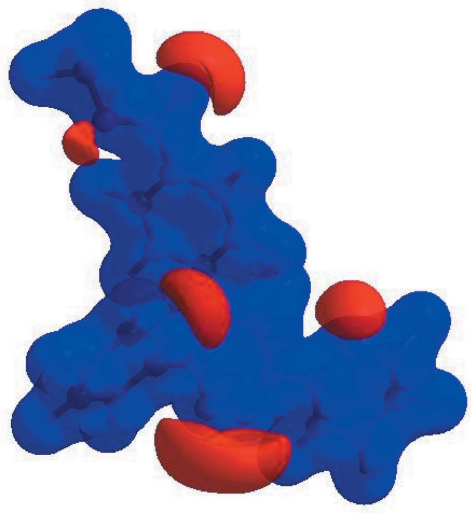

Figure 4
View of the three-dimensional Hirshfeld surface of the title compound plotted over the electrostatic potential energy in the range −0.0500 to 0.0500 a.u. using the STO-3G basis set at the Hartree–Fock level of theory. Hydrogen-bond donors and acceptors are shown as blue and red regions around the atoms corresponding to positive and negative potentials, respectively.

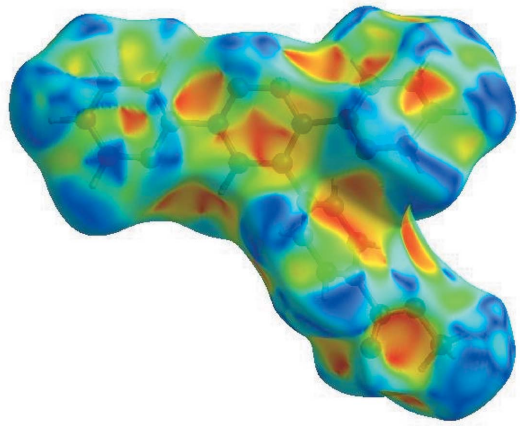

Figure 5
Hirshfeld surface of the title compound plotted over shape-index.

surface indicates contacts with distances equal to the sum of the van der Waals radii, and the red and blue colours indicate distances shorter (in close contact) or longer (distinct contact) than the van der Waals radii, respectively (Venkatesan *et al.*, 2016). The bright-red spots appearing near atoms O1 and H22*B* and H22*C* indicate their roles as the respective donors and/or acceptors; they also appear as blue and red regions corresponding to positive and negative potentials on the HS mapped over electrostatic potential (Spackman *et al.*, 2008; Jayatilaka *et al.*, 2005), as shown in Fig. 4. The blue regions indicate the positive electrostatic potential (hydrogen-bond donors), while the red regions indicate the negative electrostatic potential (hydrogen-bond acceptors). The shape-index of the HS is a tool to visualize the π–π stacking by the presence of adjacent red and blue triangles; if there are no adjacent red and/or blue triangles, then there are no π–π interactions. Fig. 5 clearly suggests that there are no π—π interactions in (I). The overall two-dimensional fingerprint plot (Fig. 6*a*) and those delineated into H···H, H···C/C···H, H···N/N···H, H···O/O···H, C···C and C···N/N···C contacts (McKinnon *et al.*, 2007) are illustrated in Figs. 6 (*b*)–(*g*), respectively, together with their relative contributions to the Hirshfeld surface. The most important interaction is H···H contributing 39.7% to the overall crystal packing, which is reflected in Fig. 6(*b*) as widely scattered points of high density due to the large hydrogen content of the molecule with the tip at $d_e = d_i = 1.10$ Å, due to the short interatomic H···H contacts (Table 2). Due to the presence of C—H···π interactions, a 27.5% contribution to the HS arises from the H···C/C···H contacts (Table 2) which are viewed as pairs of spikes in the fingerprint plot shown in Fig. 6(*c*) with the tips at $d_e + d_i = 2.75$ Å. The pair of scattered points of wings resulting in the fingerprint plots delineated into H···N/N···H (Fig. 6*d*) contacts, with a 15.5% contribution to the HS, has a symmetrical distribution of points with the edges at $d_e + d_i = 2.58$ Å (Table 2). The pair of characteristic wings resulting in the fingerprint plot shown in Fig. 6(*e*), with an 11.1% contribution to the HS, arises from the O···H/H···O contacts (Table 2) and is viewed as pair of spikes with the tips at $d_e + d_i = 2.42$ Å. The C···C contacts (Fig. 6*f*) have an arrow-shaped distribution of

Table 3
Comparison of selected (X-ray and DFT) geometric data (Å, °).

Bonds/angles	X-ray	B3LYP/6-311G(d,p)
O1—C21	1.2049 (14)	1.23831
O2—C21	1.3342 (15)	1.38677
O2—C22	1.4501 (14)	1.45892
N1—C1	1.3411 (16)	1.38974
N1—C5	1.3461 (15)	1.40690
N2—C6	1.3366 (15)	1.36917
N2—N3	1.3407 (14)	1.31753
N3—C9	1.3375 (14)	1.38785
N4—C14	1.3388 (17)	1.34410
N4—C10	1.3429 (15)	1.35601
C21—O2—C22	115.72 (9)	116.46416
C1—N1—C5	116.73 (10)	117.59335
C6—N2—N3	119.41 (9)	118.73596
C9—N3—N2	120.51 (9)	121.63356
C14—N4—C10	117.22 (11)	118.30113
N1—C5—C4	123.17 (11)	123.94848
N1—C5—C6	115.74 (10)	116.62957
N2—C6—C7	122.43 (10)	122.86465
N2—C6—C5	115.74 (10)	115.11012

points with the tip at $d_e = d_i = 13.50$ Å. Finally, the tiny characteristic wings resulting in the fingerprint plots shown in Fig. 6*g*, a 2.4% contribution to the HS, arises from the C···N/N···C contacts (Table 2) and is viewed with the tip at $d_e = d_i = 3.40$ Å.

The Hirshfeld surface representations with the function d_{norm} plotted onto the surface are shown for the H···H, H···C/C···H, H···N/N···H and H···O/O···H interactions in Figs. 7(*a*)–(*d*), respectively.

The Hirshfeld surface analysis confirms the importance of H-atom contacts in establishing the packing. The large number of H···H, H···C/C···H, H···N/N···H and H···O/O···H interactions suggest that van der Waals interactions and hydrogen bonding play the major roles in the crystal packing (Hathwar *et al.*, 2015).

5. Interaction energy calculations

The intermolecular interaction energies were calculated using the CE–B3LYP/6-31G(d,p) energy model available in *CrystalExplorer* (CE) (Version 17.5; Turner *et al.*, 2017), where a cluster of molecules would need to be generated by applying crystallographic symmetry operations with respect to a selected central molecule within a default radius of 3.8 Å (Turner *et al.*, 2014). The total intermolecular energy (E_{tot}) is the sum of the electrostatic (E_{ele}), polarization (E_{pol}), dispersion (E_{dis}) and exchange–repulsion (E_{rep}) energies (Turner *et*

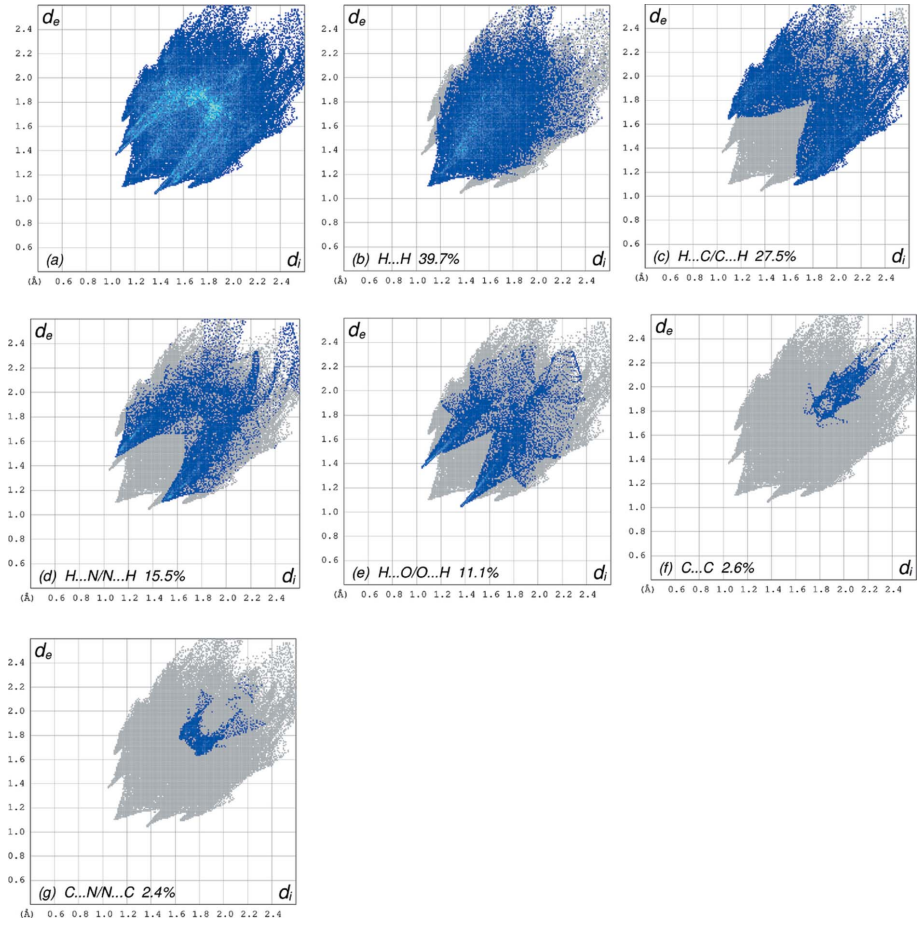

Figure 6
The full two-dimensional fingerprint plots for the title compound, showing (*a*) all interactions, and delineated into (*b*) H···H, (*c*) H···C/C···H, (*d*) H···N/N···H, (*e*) H···O/O···H, (*f*) C···C and (*g*) C···N/N···C interactions. The d_i and d_e values are the closest internal and external distances (in Å) from given points on the Hirshfeld surface contacts.

al., 2015), with scale factors of 1.057, 0.740, 0.871 and 0.618, respectively (Mackenzie *et al.*, 2017). Hydrogen-bonding interaction energies (in kJ mol^{-1}) were calculated as −23.9 (E_{ele}), −4.3 (E_{pol}), −76.2 (E_{dis}), 53.0 (E_{rep}) and −62.0 (E_{tot}) for the C22—H22*C*···O1 hydrogen-bonding interaction, and −22.0 (E_{ele}), −8.5 (E_{pol}), −28.5 (E_{dis}), 32.3 (E_{rep}) and −34.3 (E_{tot}) for the C22—H22*B*···O1 hydrogen-bonding interaction.

6. DFT calculations

The optimized structure of the title compound, (I), in the gas phase was generated theoretically *via* density functional theory (DFT) using the standard B3LYP functional and 6-311G(d,p) basis-set calculations (Becke, 1993) as implemented in *GAUSSIAN09* (Frisch *et al.*, 2009). The theoretical and experimental results are in good agreement (Table 3). The highest-occupied molecular orbital (HOMO), acting as an electron donor, and the lowest-unoccupied molecular orbital (LUMO), acting as an electron acceptor, are very important parameters for quantum chemistry. When the energy gap is small, the molecule is highly polarizable and has high chemical reactivity. The DFT calculations provide some important information on the reactivity and site selectivity of the molecular framework. E_{HOMO} and E_{LUMO} clarify the inevitable charge exchange collaboration inside the studied material, and electronegativity (χ), hardness (η), potential (μ), electrophilicity (ω) and softness (σ) are all recorded in Table 4. The significance of η and σ is to evaluate both the reactivity and stability. The electron transition from the HOMO to the LUMO energy level is shown in Fig. 8. The HOMO and LUMO are localized in the plane extending from the whole methyl 4-[3,6-bis(pyridin-2-yl)pyridazin-4-yl]benzoate ring. The energy band gap [$\Delta E = E_{LUMO} - E_{HOMO}$] of the molecule is about 1.8908 eV, and the frontier molecular orbital (FMO) energies, *i.e.* E_{HOMO} and E_{LUMO}, are −4.3680 and −2.4772 eV, respectively.

Table 4
Calculated energies.

Molecular Energy (a.u.) (eV)	Compound (I)
Total Energy *TE* (eV)	−33114.5851
E_{HOMO} (eV)	−4.3680
E_{LUMO} (eV)	−2.4772
Gap ΔE (eV)	1.8908
Dipole moment μ (Debye)	5.0683
Ionization potential *I* (eV)	4.3680
Electron affinity *A*	2.4772
Electronegativity χ	3.4226
Hardness η	0.9454
Electrophilicity index ω	6.1953
Softness σ	1.0577
Fraction of electron transferred ΔN	1.8920

7. Database survey

A 4-[(prop-2-en-1-yloxy)methyl]phenyl analogue has been reported (Filali *et al.*, 2019*a*). Three other metal complexes coordinated by 3,6-bis(pyridin-2-yl)pyridazine have also been reported, namely aquabis[3,6-bis(pyridin-2-yl)pyridazine-

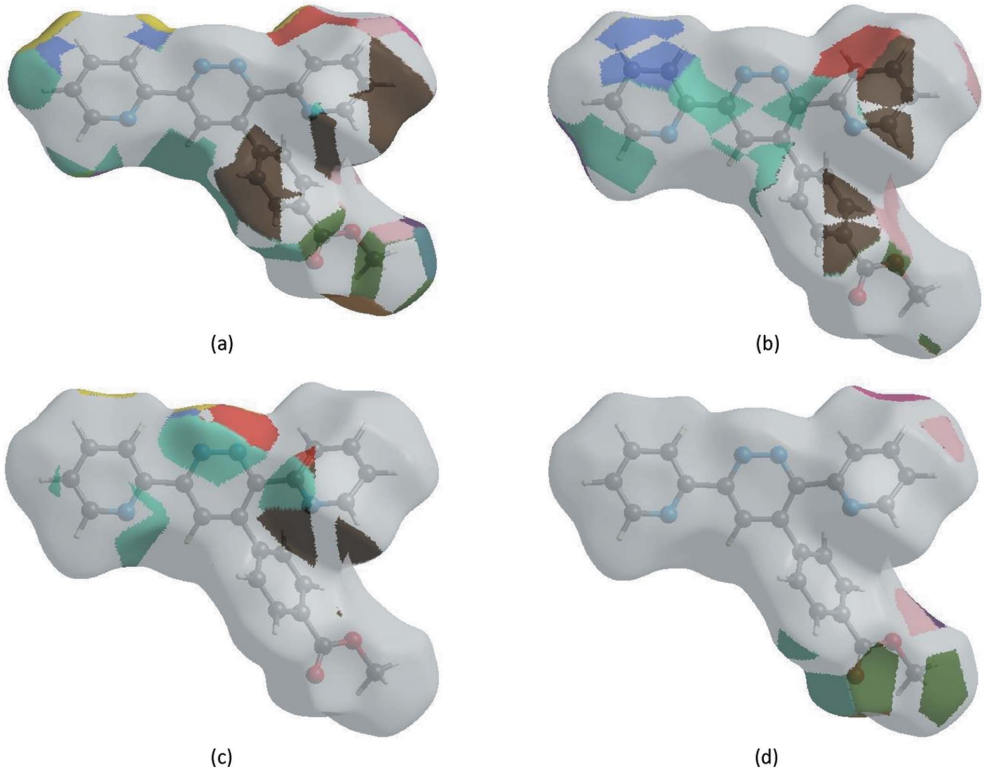

Figure 7
The Hirshfeld surface representations with the function d_{norm} plotted onto the surface for (*a*) H···H, (*b*) H···C/C···H, (*c*) H···N/N···H and (*d*) H···O/O···H interactions.

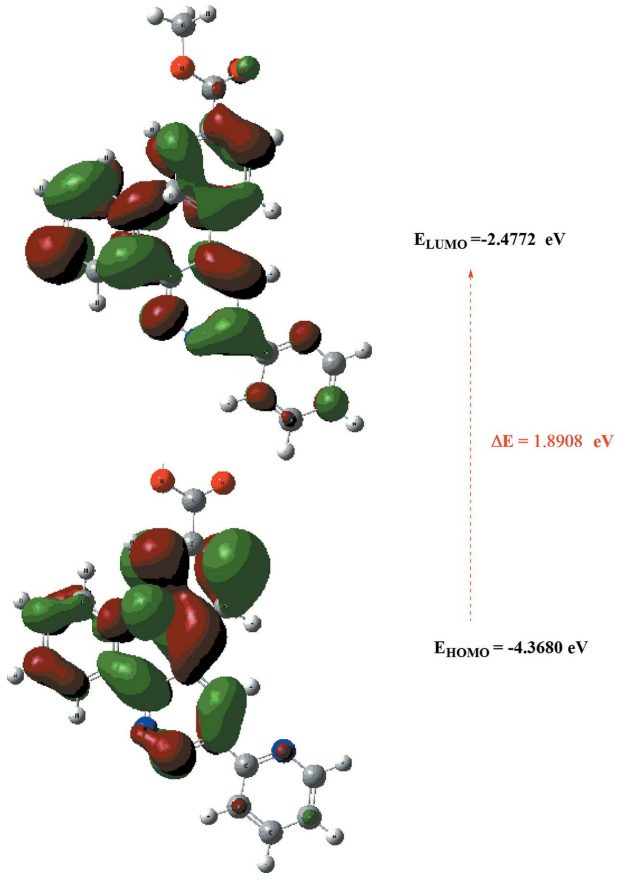

Figure 8
The energy band gap of the title compound.

κ^2N^1,N^6]copper(II) bis(trifluoromethanesulfonate) (Showrilu *et al.*, 2017), tetrakis[μ-3,6-di(pyridin-2-yl)pyridazine]bis(μ-hydroxo)bis(μ-aqua)tetranickel(II) hexanitrate tetradecahydrate (Marino *et al.*, 2019) and *catena*-[[μ_2-3,6-bis(pyridin-2-yl)pyridazine]bis(μ-2-azido)dizaidodicopper monohydrate] (Mastropietro *et al.*, 2013).

8. Synthesis and crystallization

3,6-Bis(pyridin-2-yl)-1,2,4,5-tetrazine (4 mmol) was dissolved in toluene (20 ml), and then 1 equiv. of methyl 4-ethynylbenzoate was added and the reaction mixture was stirred and refluxed at temperatures between 413 and 453 K. The solvent was then evaporated. The product obtained was separated by chromatography on a column of silica gel. The isolated solid was recrystallized from hexane–dichloromethane (1:1 *v*/*v*) to afford colourless crystals (yield 92%; m.p. 449 K).

9. Refinement

The experimental details including the crystal data, data collection and refinement are summarized in Table 5. H atoms were located in a difference Fourier map and refined freely.

Table 5
Experimental details.

Crystal data	
Chemical formula	$C_{22}H_{16}N_4O_2$
M_r	368.39
Crystal system, space group	Triclinic, $P\overline{1}$
Temperature (K)	150
a, b, c (Å)	6.0464 (1), 11.7175 (3), 13.2931 (3)
α, β, γ (°)	95.735 (1), 95.813 (1), 101.780 (1)
V (Å^3)	910.16 (3)
Z	2
Radiation type	Cu $K\alpha$
μ (mm^{-1})	0.72
Crystal size (mm)	0.26 × 0.12 × 0.07
Data collection	
Diffractometer	Bruker D8 VENTURE PHOTON 100 CMOS
Absorption correction	Multi-scan (*SADABS*; Krause *et al.*, 2015)
T_{min}, T_{max}	0.85, 0.95
No. of measured, independent and observed [$I > 2\sigma(I)$] reflections	7056, 3426, 3139
R_{int}	0.022
(sin $\theta/\lambda)_{max}$ (Å^{-1})	0.625
Refinement	
$R[F^2 > 2\sigma(F^2)]$, $wR(F^2)$, S	0.036, 0.098, 1.02
No. of reflections	3426
No. of parameters	318
H-atom treatment	All H-atom parameters refined
$\Delta\rho_{max}$, $\Delta\rho_{min}$ (e Å^{-3})	0.23, −0.17

Computer programs: *APEX3* (Bruker, 2016), *SAINT* (Bruker, 2016), *SAINT* (Bruker, 2016), *SHELXT* (Sheldrick, 2015*a*), *SHELXL2018* (Sheldrick, 2015*b*), *DIAMOND* (Brandenburg & Putz, 2012) and *SHELXTL* (Bruker, 2016).

Acknowledgements

The support of NSF-MRI for the purchase of the diffractometer and Tulane University for support of the Tulane Crystallography Laboratory are gratefully acknowledged.

Funding information

Funding for this research was provided by: Hacettepe University Scientific Research Project Unit (grant No. 013 D04 602 004 to TH); NSF-MRI (grant No. 1228232).

References

Becke, A. D. (1993). *J. Chem. Phys.* **98**, 5648–5652.
Brandenburg, K. & Putz, H. (2012). *DIAMOND*. Crystal Impact GbR, Bonn, Germany.
Bruker (2016). *APEX3*, *SAINT*, *SADABS* and *SHELXTL*. Bruker AXS Inc., Madison, Wisconsin, USA.
Filali, M., Elmsellem, H., Hökelek, T., El-Ghayoury, A., Stetsiuk, O., El Hadrami, E. M. & Ben-Tama, A. (2019*b*). *Acta Cryst.* E**75**, 1169–1174.
Filali, M., Sebbar, N. K., Hökelek, T., Mague, J. T., Chakroune, S., Ben-Tama, A. & El Hadrami, E. M. (2019*a*). *Acta Cryst.* E**75**, 1321–1326.
Frisch, M. J., *et al.* (2009). *GAUSSIAN09*. Gaussian Inc., Wallingford, CT, USA.
Hathwar, V. R., Sist, M., Jørgensen, M. R. V., Mamakhel, A. H., Wang, X., Hoffmann, C. M., Sugimoto, K., Overgaard, J. & Iversen, B. B. (2015). *IUCrJ*, **2**, 563–574.
Hirshfeld, H. L. (1977). *Theor. Chim. Acta*, **44**, 129–138.

Jayatilaka, D., Grimwood, D. J., Lee, A., Lemay, A., Russel, A. J., Taylor, C., Wolff, S. K., Cassam-Chenai, P. & Whitton, A. (2005). *TONTO – A System for Computational Chemistry*. Available at: http://hirshfeldsurface.net/.
Kaim, W. & Kohlmann, S. (1987). *Inorg. Chem.* **26**, 68–77.
Khadiri, A., Saddik, R., Bekkouche, K., Aouniti, A., Hammouti, B., Benchat, N., Bouachrine, M. & Solmaz, R. (2016). *J. Taiwan Inst. Chem. Eng.* **58**, 552–564.
Kore, A. R., Yang, B. & Srinivasan, B. (2015). *Tetrahedron Lett.* **56**, 808–811.
Krause, L., Herbst-Irmer, R., Sheldrick, G. M. & Stalke, D. (2015). *J. Appl. Cryst.* **48**, 3–10.
Mackenzie, C. F., Spackman, P. R., Jayatilaka, D. & Spackman, M. A. (2017). *IUCrJ*, **4**, 575–587.
Marino, N., Bruno, R., Bentama, A., Pascual-Álvarez, A., Lloret, F., Julve, M. & De Munno, G. (2019). *CrystEngComm*, **21**, 917–924.
Mastropietro, T. F., Marino, N., Armentano, D., De Munno, G., Yuste, C., Lloret, F. & Julve, M. (2013). *Cryst. Growth Des.* **13**, 270–281.
McKinnon, J. J., Jayatilaka, D. & Spackman, M. A. (2007). *Chem. Commun.* pp. 3814.
Sheldrick, G. M. (2015*a*). *Acta Cryst.* A**71**, 3–8.
Sheldrick, G. M. (2015*b*). *Acta Cryst.* C**71**, 3–8.
Showrilu, K., Rajarajan, K., Martin Britto Dhas, S. A. & Athimoolam, S. (2017). *IUCrData*, **2**, x171142.
Spackman, M. A. & Jayatilaka, D. (2009). *CrystEngComm*, **11**, 19–32.
Spackman, M. A., McKinnon, J. J. & Jayatilaka, D. (2008). *CrystEngComm*, **10**, 377–388.
Tsukada, N., Sato, T., Mori, H., Sugawara, S., Kabuto, C., Miyano, S. & Inoue, Y. (2001). *J. Organomet. Chem.* **627**, 121–126.
Turner, M. J., Grabowsky, S., Jayatilaka, D. & Spackman, M. A. (2014). *J. Phys. Chem. Lett.* **5**, 4249–4255.
Turner, M. J., McKinnon, J. J., Wolff, S. K., Grimwood, D. J., Spackman, P. R., Jayatilaka, D. & Spackman, M. A. (2017). *CrystalExplorer17*. The University of Western Australia.
Turner, M. J., Thomas, S. P., Shi, M. W., Jayatilaka, D. & Spackman, M. A. (2015). *Chem. Commun.* **51**, 3735–3738.
Venkatesan, P., Thamotharan, S., Ilangovan, A., Liang, H. & Sundius, T. (2016). *Spectrochim. Acta A Mol. Biomol. Spectrosc.* **153**, 625–636.

supporting information

Acta Cryst. (2019). E**75**, 1672-1678 [https://doi.org/10.1107/S2056989019013732]

Crystal structure, Hirshfeld surface analysis and interaction energy and DFT studies of methyl 4-[3,6-bis(pyridin-2-yl)pyridazin-4-yl]benzoate

Mouad Filali, Lhoussaine El Ghayati, Tuncer Hökelek, Joel T. Mague, Abdessalam Ben-Tama, El Mestafa El Hadrami and Nada Kheira Sebbar

Computing details

Data collection: *APEX3* (Bruker, 2016); cell refinement: *SAINT* (Bruker, 2016); data reduction: *SAINT* (Bruker, 2016); program(s) used to solve structure: *SHELXT* (Sheldrick, 2015*a*); program(s) used to refine structure: *SHELXL2018* (Sheldrick, 2015*b*); molecular graphics: *DIAMOND* (Brandenburg & Putz, 2012); software used to prepare material for publication: *SHELXTL* (Bruker, 2016).

Methyl 4-[3,6-bis(pyridin-2-yl)pyridazin-4-yl]benzoate

Crystal data

$C_{22}H_{16}N_4O_2$
$M_r = 368.39$
Triclinic, $P\overline{1}$
$a = 6.0464$ (1) Å
$b = 11.7175$ (3) Å
$c = 13.2931$ (3) Å
$\alpha = 95.735$ (1)°
$\beta = 95.813$ (1)°
$\gamma = 101.780$ (1)°
$V = 910.16$ (3) Å^3
$Z = 2$
$F(000) = 384$
$D_x = 1.344$ Mg m^{-3}
Cu $K\alpha$ radiation, $\lambda = 1.54178$ Å
Cell parameters from 6104 reflections
$\theta = 3.4$–74.7°
$\mu = 0.72$ mm^{-1}
$T = 150$ K
Column, colourless
0.26 × 0.12 × 0.07 mm

Data collection

Bruker D8 VENTURE PHOTON 100 CMOS diffractometer
Radiation source: INCOATEC IμS micro-focus source
Mirror monochromator
Detector resolution: 10.4167 pixels mm^{-1}
ω scans
Absorption correction: multi-scan (*SADABS*; Krause *et al.*, 2015)
$T_{min} = 0.85$, $T_{max} = 0.95$
7056 measured reflections
3426 independent reflections
3139 reflections with $I > 2\sigma(I)$
$R_{int} = 0.022$
$\theta_{max} = 74.7°$, $\theta_{min} = 3.4°$
$h = -6\rightarrow7$
$k = -14\rightarrow13$
$l = -14\rightarrow16$

Refinement

Refinement on F^2
Least-squares matrix: full
$R[F^2 > 2\sigma(F^2)] = 0.036$
$wR(F^2) = 0.098$
$S = 1.02$
3426 reflections
318 parameters
0 restraints
Primary atom site location: dual space
Secondary atom site location: difference Fourier map
Hydrogen site location: difference Fourier map

All H-atom parameters refined
$w = 1/[\sigma^2(F_o^2) + (0.0539P)^2 + 0.2048P]$ where $P = (F_o^2 + 2F_c^2)/3$
$(\Delta/\sigma)_{max} < 0.001$
$\Delta\rho_{max} = 0.23$ e Å^{-3}
$\Delta\rho_{min} = -0.16$ e Å^{-3}
Extinction correction: *SHELXL2018* (Sheldrick, 2015*b*), $Fc^* = kFc[1+0.001xFc^2\lambda^3/\sin(2\theta)]^{-1/4}$
Extinction coefficient: 0.0087 (8)

Special details

Geometry. All esds (except the esd in the dihedral angle between two l.s. planes) are estimated using the full covariance matrix. The cell esds are taken into account individually in the estimation of esds in distances, angles and torsion angles; correlations between esds in cell parameters are only used when they are defined by crystal symmetry. An approximate (isotropic) treatment of cell esds is used for estimating esds involving l.s. planes.

Refinement. Refinement of F^2 against ALL reflections. The weighted R-factor wR and goodness of fit S are based on F^2, conventional R-factors R are based on F, with F set to zero for negative F^2. The threshold expression of $F^2 > 2\text{sigma}(F^2)$ is used only for calculating R-factors(gt) etc. and is not relevant to the choice of reflections for refinement. R-factors based on F^2 are statistically about twice as large as those based on F, and R- factors based on ALL data will be even larger.

Fractional atomic coordinates and isotropic or equivalent isotropic displacement parameters (Å²)

	x	*y*	*z*	U_{iso}*/U_{eq}
O1	0.62576 (15)	0.94764 (7)	0.85874 (8)	0.0425 (3)
O2	0.24890 (14)	0.87662 (7)	0.83965 (7)	0.0313 (2)
N1	1.02078 (16)	0.30995 (9)	0.51060 (7)	0.0290 (2)
N2	0.52919 (17)	0.16735 (8)	0.61309 (8)	0.0294 (2)
N3	0.38764 (17)	0.18823 (8)	0.68071 (8)	0.0292 (2)
N4	0.32230 (18)	0.39009 (9)	0.87963 (8)	0.0328 (2)
C1	1.1730 (2)	0.28112 (11)	0.45151 (9)	0.0319 (3)
H1	1.308 (3)	0.3455 (14)	0.4491 (12)	0.041 (4)*
C2	1.1492 (2)	0.17134 (12)	0.39688 (10)	0.0352 (3)
H2	1.270 (3)	0.1577 (15)	0.3566 (14)	0.053 (5)*
C3	0.9553 (2)	0.08688 (11)	0.40089 (10)	0.0361 (3)
H3	0.929 (3)	0.0079 (15)	0.3616 (13)	0.047 (4)*
C4	0.7948 (2)	0.11428 (11)	0.46092 (9)	0.0325 (3)
H4	0.656 (3)	0.0587 (15)	0.4647 (12)	0.047 (4)*
C5	0.83537 (19)	0.22568 (10)	0.51552 (8)	0.0263 (2)
C6	0.67584 (19)	0.25744 (10)	0.58616 (8)	0.0258 (2)
C7	0.67982 (19)	0.37445 (10)	0.62177 (9)	0.0264 (2)
H7	0.783 (2)	0.4381 (13)	0.5971 (11)	0.031 (3)*
C8	0.53152 (19)	0.39724 (9)	0.68926 (8)	0.0253 (2)
C9	0.38988 (19)	0.29823 (10)	0.71976 (8)	0.0257 (2)
C10	0.2376 (2)	0.30746 (9)	0.79999 (9)	0.0267 (2)
C11	0.0258 (2)	0.23148 (10)	0.79314 (9)	0.0297 (3)
H11	−0.027 (3)	0.1701 (13)	0.7335 (12)	0.037 (4)*
C12	−0.1065 (2)	0.24211 (11)	0.87157 (10)	0.0356 (3)
H12	−0.260 (3)	0.1895 (14)	0.8668 (12)	0.042 (4)*
C13	−0.0224 (3)	0.32801 (12)	0.95334 (11)	0.0398 (3)
H13	−0.111 (3)	0.3385 (15)	1.0109 (14)	0.050 (4)*
C14	0.1922 (2)	0.39898 (11)	0.95456 (10)	0.0386 (3)
H14	0.258 (3)	0.4584 (14)	1.0115 (13)	0.042 (4)*
C15	0.51538 (18)	0.51941 (9)	0.72438 (8)	0.0245 (2)

C16	0.70032 (19)	0.59753 (10)	0.78141 (9)	0.0264 (2)
H16	0.839 (2)	0.5708 (12)	0.7993 (11)	0.032 (3)*
C17	0.68255 (19)	0.71046 (10)	0.81609 (9)	0.0273 (3)
H17	0.807 (2)	0.7636 (13)	0.8570 (11)	0.033 (4)*
C18	0.47906 (18)	0.74593 (9)	0.79418 (8)	0.0247 (2)
C19	0.29575 (19)	0.66908 (10)	0.73420 (9)	0.0277 (3)
H19	0.157 (3)	0.6959 (12)	0.7180 (11)	0.032 (4)*
C20	0.3147 (2)	0.55664 (10)	0.69887 (9)	0.0290 (3)
H20	0.188 (3)	0.5009 (13)	0.6556 (12)	0.039 (4)*
C21	0.46364 (19)	0.86730 (10)	0.83384 (9)	0.0271 (3)
C22	0.2179 (2)	0.99301 (11)	0.87423 (12)	0.0371 (3)
H22A	0.289 (3)	1.0486 (15)	0.8283 (13)	0.046 (4)*
H22B	0.287 (3)	1.0160 (15)	0.9439 (14)	0.050 (5)*
H22C	0.056 (3)	0.9847 (15)	0.8673 (13)	0.051 (5)*

Atomic displacement parameters (Å²)

	U^{11}	U^{22}	U^{33}	U^{12}	U^{13}	U^{23}
O1	0.0280 (5)	0.0261 (4)	0.0677 (7)	0.0017 (3)	0.0007 (4)	−0.0079 (4)
O2	0.0264 (4)	0.0246 (4)	0.0426 (5)	0.0066 (3)	0.0043 (3)	−0.0004 (3)
N1	0.0270 (5)	0.0304 (5)	0.0283 (5)	0.0045 (4)	0.0007 (4)	0.0036 (4)
N2	0.0324 (5)	0.0247 (5)	0.0304 (5)	0.0045 (4)	0.0059 (4)	0.0012 (4)
N3	0.0324 (5)	0.0245 (5)	0.0303 (5)	0.0051 (4)	0.0064 (4)	0.0019 (4)
N4	0.0401 (6)	0.0282 (5)	0.0282 (5)	0.0031 (4)	0.0064 (4)	0.0018 (4)
C1	0.0281 (6)	0.0389 (6)	0.0290 (6)	0.0067 (5)	0.0029 (4)	0.0080 (5)
C2	0.0381 (7)	0.0427 (7)	0.0303 (6)	0.0165 (5)	0.0098 (5)	0.0089 (5)
C3	0.0479 (8)	0.0306 (6)	0.0320 (6)	0.0125 (5)	0.0098 (5)	0.0021 (5)
C4	0.0373 (7)	0.0275 (6)	0.0319 (6)	0.0046 (5)	0.0072 (5)	0.0017 (5)
C5	0.0271 (6)	0.0260 (5)	0.0256 (6)	0.0060 (4)	0.0008 (4)	0.0033 (4)
C6	0.0254 (6)	0.0254 (5)	0.0252 (5)	0.0047 (4)	−0.0007 (4)	0.0016 (4)
C7	0.0249 (6)	0.0237 (5)	0.0287 (6)	0.0026 (4)	0.0005 (4)	0.0028 (4)
C8	0.0245 (5)	0.0238 (5)	0.0260 (5)	0.0048 (4)	−0.0018 (4)	0.0017 (4)
C9	0.0261 (6)	0.0241 (5)	0.0258 (5)	0.0046 (4)	0.0000 (4)	0.0023 (4)
C10	0.0305 (6)	0.0232 (5)	0.0273 (6)	0.0074 (4)	0.0031 (4)	0.0049 (4)
C11	0.0294 (6)	0.0261 (5)	0.0339 (6)	0.0076 (4)	0.0024 (5)	0.0040 (5)
C12	0.0304 (7)	0.0352 (6)	0.0436 (7)	0.0084 (5)	0.0089 (5)	0.0090 (5)
C13	0.0460 (8)	0.0393 (7)	0.0382 (7)	0.0124 (6)	0.0165 (6)	0.0066 (5)
C14	0.0496 (8)	0.0340 (6)	0.0312 (6)	0.0060 (6)	0.0102 (5)	0.0009 (5)
C15	0.0256 (6)	0.0221 (5)	0.0253 (5)	0.0032 (4)	0.0042 (4)	0.0035 (4)
C16	0.0222 (6)	0.0258 (5)	0.0307 (6)	0.0050 (4)	0.0019 (4)	0.0038 (4)
C17	0.0232 (6)	0.0245 (5)	0.0313 (6)	0.0014 (4)	0.0001 (4)	0.0014 (4)
C18	0.0249 (6)	0.0218 (5)	0.0268 (5)	0.0033 (4)	0.0039 (4)	0.0031 (4)
C19	0.0226 (6)	0.0263 (5)	0.0333 (6)	0.0051 (4)	0.0007 (4)	0.0029 (4)
C20	0.0248 (6)	0.0251 (5)	0.0336 (6)	0.0021 (4)	−0.0021 (4)	−0.0004 (4)
C21	0.0252 (6)	0.0253 (5)	0.0299 (6)	0.0045 (4)	0.0015 (4)	0.0026 (4)
C22	0.0339 (7)	0.0291 (6)	0.0484 (8)	0.0116 (5)	0.0040 (6)	−0.0034 (6)

Geometric parameters (Å, º)

O1—C21	1.2049 (14)	C9—C10	1.4876 (16)
O2—C21	1.3342 (15)	C10—C11	1.3914 (17)
O2—C22	1.4501 (14)	C11—C12	1.3877 (18)
N1—C1	1.3411 (16)	C11—H11	0.994 (15)
N1—C5	1.3461 (15)	C12—C13	1.3833 (19)
N2—C6	1.3366 (15)	C12—H12	0.996 (16)
N2—N3	1.3407 (14)	C13—C14	1.389 (2)
N3—C9	1.3375 (14)	C13—H13	0.989 (18)
N4—C14	1.3388 (17)	C14—H14	0.968 (16)
N4—C10	1.3429 (15)	C15—C16	1.3909 (15)
C1—C2	1.3854 (18)	C15—C20	1.3926 (16)
C1—H1	0.998 (16)	C16—C17	1.3861 (15)
C2—C3	1.3804 (19)	C16—H16	0.967 (15)
C2—H2	0.979 (18)	C17—C18	1.3899 (16)
C3—C4	1.3837 (18)	C17—H17	0.954 (15)
C3—H3	0.990 (16)	C18—C19	1.3946 (15)
C4—C5	1.3909 (16)	C18—C21	1.4911 (15)
C4—H4	0.962 (17)	C19—C20	1.3851 (16)
C5—C6	1.4869 (16)	C19—H19	0.967 (15)
C6—C7	1.3997 (15)	C20—H20	0.987 (16)
C7—C8	1.3759 (16)	C22—H22A	1.000 (18)
C7—H7	0.975 (15)	C22—H22B	0.964 (19)
C8—C9	1.4151 (16)	C22—H22C	0.959 (19)
C8—C15	1.4864 (14)		
O2···C3^{i}	3.4089 (16)	N4···H14^{viii}	2.931 (18)
O1···H12^{ii}	2.765 (16)	C1···C6^{iii}	3.4447 (17)
O1···H22A	2.573 (18)	C1···C7^{iii}	3.5272 (17)
O1···H22B	2.660 (18)	C2···C17^{ix}	3.4292 (18)
O1···H22C^{iii}	2.537 (19)	C3···C3^{x}	3.5516 (18)
O1···H22B^{iv}	2.598 (18)	C6···C11^{iii}	3.3751 (16)
O1···H17	2.611 (14)	C10···C20	3.3022 (16)
O2···H17^{v}	2.773 (13)	C11···C22^{vii}	3.4630 (18)
O2···H19	2.462 (14)	C14···C17^{viii}	3.4960 (18)
N1···C9^{iii}	3.4168 (15)	C14···C16^{viii}	3.4987 (18)
N2···C1^{v}	3.4404 (16)	C1···H19^{i}	2.926 (16)
N4···C20	3.2459 (16)	C6···H11^{iii}	2.924 (15)
N4···C15	2.8825 (15)	C7···H1^{v}	2.988 (17)
N4···C16	3.4362 (16)	C11···H22A^{vii}	2.964 (18)
N1···H20^{iii}	2.750 (15)	C16···H14^{viii}	2.891 (17)
N1···H7	2.553 (14)	C17···H2^{ix}	2.898 (18)
N2···H4^{vi}	2.710 (17)	C18···H2^{ix}	2.822 (18)
N2···H4	2.511 (17)	H3···H11^{vi}	2.53 (2)
N3···H11	2.644 (13)	H4···H4^{vi}	2.43 (3)
N3···H22A^{vii}	2.713 (17)	H7···H20^{iii}	2.43 (2)
N3···H3^{vi}	2.644 (18)	H16···H19^{iii}	2.57 (2)

C21—O2—C22	115.72 (9)	C10—C11—H11	120.0 (9)
C1—N1—C5	116.73 (10)	C13—C12—C11	118.62 (12)
C6—N2—N3	119.41 (9)	C13—C12—H12	121.9 (9)
C9—N3—N2	120.51 (9)	C11—C12—H12	119.5 (9)
C14—N4—C10	117.22 (11)	C12—C13—C14	118.80 (12)
N1—C1—C2	123.85 (11)	C12—C13—H13	121.2 (10)
N1—C1—H1	114.9 (9)	C14—C13—H13	120.0 (10)
C2—C1—H1	121.3 (9)	N4—C14—C13	123.44 (12)
C3—C2—C1	118.61 (11)	N4—C14—H14	115.5 (10)
C3—C2—H2	123.1 (10)	C13—C14—H14	121.0 (9)
C1—C2—H2	118.3 (10)	C16—C15—C20	119.63 (10)
C2—C3—C4	118.80 (12)	C16—C15—C8	120.52 (10)
C2—C3—H3	121.6 (10)	C20—C15—C8	119.84 (10)
C4—C3—H3	119.6 (10)	C17—C16—C15	120.28 (10)
C3—C4—C5	118.79 (12)	C17—C16—H16	120.5 (8)
C3—C4—H4	121.6 (10)	C15—C16—H16	119.1 (8)
C5—C4—H4	119.6 (10)	C16—C17—C18	119.99 (10)
N1—C5—C4	123.17 (11)	C16—C17—H17	120.6 (9)
N1—C5—C6	115.74 (10)	C18—C17—H17	119.4 (9)
C4—C5—C6	121.07 (10)	C17—C18—C19	119.84 (10)
N2—C6—C7	122.43 (10)	C17—C18—C21	118.84 (10)
N2—C6—C5	115.74 (10)	C19—C18—C21	121.31 (10)
C7—C6—C5	121.82 (10)	C20—C19—C18	120.00 (10)
C8—C7—C6	118.68 (10)	C20—C19—H19	121.2 (8)
C8—C7—H7	121.2 (8)	C18—C19—H19	118.8 (8)
C6—C7—H7	120.1 (8)	C19—C20—C15	120.17 (10)
C7—C8—C9	116.35 (10)	C19—C20—H20	121.7 (9)
C7—C8—C15	121.43 (10)	C15—C20—H20	118.2 (9)
C9—C8—C15	122.17 (10)	O1—C21—O2	123.69 (10)
N3—C9—C8	122.45 (10)	O1—C21—C18	124.18 (10)
N3—C9—C10	114.54 (10)	O2—C21—C18	112.13 (9)
C8—C9—C10	122.98 (10)	O2—C22—H22A	108.3 (9)
N4—C10—C11	123.19 (11)	O2—C22—H22B	109.6 (10)
N4—C10—C9	115.56 (10)	H22A—C22—H22B	111.1 (14)
C11—C10—C9	121.21 (10)	O2—C22—H22C	104.1 (10)
C12—C11—C10	118.71 (11)	H22A—C22—H22C	111.1 (14)
C12—C11—H11	121.3 (9)	H22B—C22—H22C	112.3 (15)

C6—N2—N3—C9	1.13 (16)	N3—C9—C10—C11	−37.56 (15)
C5—N1—C1—C2	−0.15 (17)	C8—C9—C10—C11	144.40 (12)
N1—C1—C2—C3	1.69 (19)	N4—C10—C11—C12	0.83 (18)
C1—C2—C3—C4	−1.34 (19)	C9—C10—C11—C12	178.28 (10)
C2—C3—C4—C5	−0.40 (19)	C10—C11—C12—C13	0.11 (18)
C1—N1—C5—C4	−1.75 (17)	C11—C12—C13—C14	−1.0 (2)
C1—N1—C5—C6	176.55 (10)	C10—N4—C14—C13	−0.2 (2)
C3—C4—C5—N1	2.05 (19)	C12—C13—C14—N4	1.1 (2)
C3—C4—C5—C6	−176.17 (11)	C7—C8—C15—C16	−64.14 (15)

N3—N2—C6—C7	−3.53 (17)	C9—C8—C15—C16	118.48 (12)
N3—N2—C6—C5	176.55 (9)	C7—C8—C15—C20	114.96 (12)
N1—C5—C6—N2	−162.08 (10)	C9—C8—C15—C20	−62.42 (15)
C4—C5—C6—N2	16.27 (16)	C20—C15—C16—C17	2.49 (17)
N1—C5—C6—C7	18.00 (16)	C8—C15—C16—C17	−178.41 (10)
C4—C5—C6—C7	−163.65 (11)	C15—C16—C17—C18	0.21 (17)
N2—C6—C7—C8	1.90 (17)	C16—C17—C18—C19	−2.31 (17)
C5—C6—C7—C8	−178.18 (10)	C16—C17—C18—C21	179.05 (10)
C6—C7—C8—C9	1.90 (16)	C17—C18—C19—C20	1.71 (17)
C6—C7—C8—C15	−175.63 (10)	C21—C18—C19—C20	−179.68 (11)
N2—N3—C9—C8	2.85 (17)	C18—C19—C20—C15	0.99 (18)
N2—N3—C9—C10	−175.20 (10)	C16—C15—C20—C19	−3.08 (17)
C7—C8—C9—N3	−4.30 (16)	C8—C15—C20—C19	177.81 (10)
C15—C8—C9—N3	173.21 (10)	C22—O2—C21—O1	2.69 (18)
C7—C8—C9—C10	173.58 (10)	C22—O2—C21—C18	−177.94 (10)
C15—C8—C9—C10	−8.91 (17)	C17—C18—C21—O1	21.65 (18)
C14—N4—C10—C11	−0.80 (18)	C19—C18—C21—O1	−156.97 (13)
C14—N4—C10—C9	−178.38 (11)	C17—C18—C21—O2	−157.72 (10)
N3—C9—C10—N4	140.07 (11)	C19—C18—C21—O2	23.66 (15)
C8—C9—C10—N4	−37.96 (15)		

Symmetry codes: (i) −*x*+1, −*y*+1, −*z*+1; (ii) *x*+1, *y*+1, *z*; (iii) *x*+1, *y*, *z*; (iv) −*x*+1, −*y*+2, −*z*+2; (v) *x*−1, *y*, *z*; (vi) −*x*+1, −*y*, −*z*+1; (vii) *x*, *y*−1, *z*; (viii) −*x*+1, −*y*+1, −*z*+2; (ix) −*x*+2, −*y*+1, −*z*+1; (x) −*x*+2, −*y*, −*z*+1.

Hydrogen-bond geometry (Å, º)

*Cg*1 is the centroid of the pyridyl ring, *A* (N1/C1–C5).

D—H···*A*	*D*—H	H···*A*	*D*···*A*	*D*—H···*A*
C19—H19···*Cg*1^{i}	0.967 (15)	2.876 (15)	3.5715 (13)	129.8 (12)
C22—H22*B*···O1^{iv}	0.964 (19)	2.598 (19)	3.5407 (19)	165.8 (14)
C22—H22*C*···O1^{v}	0.959 (19)	2.536 (19)	3.4924 (16)	174.8 (15)

Symmetry codes: (i) −*x*+1, −*y*+1, −*z*+1; (iv) −*x*+1, −*y*+2, −*z*+2; (v) *x*−1, *y*, *z*.